

**Title:** Protocol Optimization for Exosome Production from Umbilical Cord Mesenchymal Stem Cells: A Step Toward Clinical Translation

**Running title:** UC-MSC Exosomes: Standardized Production

**Authors:** Amir Bavafa<sup>1,2</sup>, Ali Sepehrinezhad<sup>1,2,\*</sup>, Ali Gorji<sup>3,4</sup>, Fatemeh Forouzanfar<sup>1,2,\*</sup>, Sajad Sahab-Negah<sup>5,\*</sup>

1. *Neuroscience Research Center, Mashhad University of Medical Sciences, Mashhad, Iran.*
2. *Department of Neuroscience, Faculty of Medicine, Mashhad University of Medical Sciences, Mashhad, Iran.*
3. *Shefa Neuroscience Research Center, Khatam Alanbia Hospital, Tehran, Iran.*
4. *Epilepsy Research Center, Department of Neurosurgery, Münster University, Münster, Germany.*
5. *Multiple Sclerosis Research Center, Neuroscience Institute, Tehran University of Medical Sciences, Tehran, Iran.*

**\*Corresponding Author:** Ali Sepehrinezhad, Fatemeh Forouzanfar, Department of Neuroscience, Faculty of Medicine, Neuroscience Research Center, Mashhad University of Medical Sciences, Mashhad, Iran. Sajad Sahab Negah, Multiple Sclerosis Research Center, Neuroscience Institute, Tehran University of Medical Sciences, Tehran, Iran. Emails: sepehrinezhada@mums.ac.ir, forouzanfarff@gmail.com, sahabnegahs@mums.ac.ir

To appear in: **Basic and Clinical Neuroscience**

**Received date:** 2025/05/30

**Revised date:** 2025/07/23

**Accepted date:** 2025/07/30

This is a “Just Accepted” manuscript, which has been examined by the peer-review process and has been accepted for publication. A “Just Accepted” manuscript is published online shortly after its acceptance, which is prior to technical editing and formatting and author proofing. *Basic and Clinical Neuroscience* provides “Just Accepted” as an optional and free service which allows authors to make their results available to the research community as soon as possible after acceptance. After a manuscript has been technically edited and formatted, it will be removed from the “Just Accepted” Web site and published as a published article. Please note that technical editing may introduce minor changes to the manuscript text and/or graphics which may affect the content, and all legal disclaimers that apply to the journal pertain.

**Please cite this article as:**

Bavafa, A., Sepehrinezhad, A., Gorji A., Forouzanfar, F., Sahab-Negah, S. (In Press). Protocol Optimization for Exosome Production from Umbilical Cord Mesenchymal Stem Cells: A Step Toward Clinical Translation. *Basic and Clinical Neuroscience*. Just Accepted publication Nov. 10, 2025. Doi: <http://dx.doi.org/10.32598/bcn.2025.2162.2>

DOI: <http://dx.doi.org/10.32598/bcn.2025.2162.2>

## Abstract

**Background:** Exosomes, nano-scale extracellular vesicles, hold transformative potential in regenerative medicine and neurodegenerative disease treatment. However, inconsistent isolation methods, contamination risks, and lack of standardization impede clinical translation. This study introduces a protocol, guided by the Minimal Information for Studies of Extracellular Vesicles (MISEV) guidelines, for isolating high-concentration exosomes from human umbilical cord mesenchymal stem cells (UC-MSCs).

**Methods:** UC-MSCs were expanded in alpha-MEM with 10% fetal bovine serum, followed by serum-free conditioning. Phenotypic characterization via flow cytometry confirmed CD90/CD44 positivity and CD45/CD11b negativity. Exosomes were isolated via differential centrifugation, filtration, and dual ultracentrifugation. Characterization was performed using transmission electron microscopy (TEM), dynamic light scattering (DLS), and bicinchoninic acid (BCA) assay, and Western blot analysis for CD9 and CD63, with calnexin as a negative control.

**Results:** TEM confirmed exosome integrity with spherical or cup-shaped morphology and intact bilayers. DLS showed a monodisperse population ( $121.3 \pm 23.7$  nm, PDI < 0.3) and stable zeta potential ( $-37.3$  to  $-43.8$  mV). The BCA assay quantified exosomal protein at  $1098.2$   $\mu$ g/mL, surpassing conventional yields. Western blot confirmed expression of CD9 and CD63 and absence of calnexin, indicating minimal contamination.

**Conclusions:** This standardized, reproducible protocol produces therapeutic-grade UC-MSC exosomes with high structural fidelity and colloidal stability, aligning with MISEV criteria. While scalability remains a challenge, the method provides a critical foundation for translational studies. Future work should prioritize functional assays in neurodegenerative models, cargo profiling, and comparative analyses with other MSC sources. This study advances exosome research toward clinical-grade applications, bridging gaps in regenerative medicine and therapeutic development.

**Keywords:** Exosomes, Mesenchymal stem cells, Ultracentrifugation, Regenerative medicine, Neurodegenerative diseases, Translational research.

## Introduction

Exosomes, extracellular vesicles with nanometer dimensions (30 to 150 nm), are known as key messengers in intercellular communication that regulate physiological balance in the body by transporting biological molecules such as proteins, RNAs, and lipids (Miron & Zhang, 2024; Xiong et al., 2024; K. Yadav et al., 2024). In the last decade, these particles have become one of the great hopes in regenerative medicine and the treatment of neurodegenerative diseases, such as Alzheimer's and Parkinson's diseases, due to their unique capabilities in repairing damaged tissues and modulating inflammatory responses (Hussen et al., 2024; Nouri et al., 2024). Studies have shown that exosomes can act as natural carriers for the delivery of therapeutic agents and provide a new approach in targeted therapy by crossing biological barriers such as the blood-brain barrier (Bai et al., 2025; Jiao et al., 2024; K. Yadav et al., 2024). These features have placed exosomes in the spotlight of advanced research and highlighted the need to develop efficient methods to exploit their therapeutic potential.

Among the diverse sources of exosomes, umbilical cord-derived mesenchymal stem cells (UC-MSCs) have gained a special place due to their exceptional properties. The advantages of these cells over other MSC sources, including non-invasive access and low immunogenicity, make them an attractive option for clinical applications (Li, Xia, Gao, Chen, & Xu, 2015). With their high proliferation capacity, potent anti-inflammatory properties, and ability to secrete regenerative factors (Jin et al., 2013), these cells are considered an ideal source for producing exosomes (Cui et al., 2024). Exosomes extracted from UC-MSCs contain neuroprotective microRNAs and proteins that play critical roles in tissue repair and the reduction of inflammation (Kang & Guo, 2022; Luan, Liu, Li, Wang, & Wang, 2024). These advantages have made UC-MSCs the focus of emerging research in exosome-based therapies.

Despite the high therapeutic potential of exosomes, several obstacles remain in translating this technology into clinical applications. Common isolation methods, such as ultracentrifugation, polymer precipitation, and size-based chromatography (SEC), are often associated with problems such as protein contamination, reduced purity, and loss of structural integrity of exosomes (Akbar, Malekian, Baghban, Kodam, & Ullah, 2022; Chen et al., 2022; Jia et al., 2022). Furthermore, the lack of universal standards for the characterization and evaluation of exosomes makes it difficult to compare results across different studies and slows down the progress of translational research (Yadav, Xuan, Sen, & Ghatak, 2024; Yin, You, Li, Li, & Guo, 2024). These challenges not only affect the quality of therapeutic exosomes but also reduce confidence in their clinical applications (Lee et al., 2024). Therefore, there is a growing need for a standardized and reliable protocol.

This study introduces the first standardized protocol compliant with the minimal information for studies of extracellular vesicles (MISEV) guidelines (Théry et al., 2018; Welsh et al., 2024; Zhang, Lan, & Chen, 2024), specifically developed for the efficient isolation of high-quality exosomes from UC-MSCs, addressing the critical need for optimized methods tailored to this unique cell source. In this way, we established a reproducible and standardized method to provide a solid foundation for translational research and pave the way for the development of novel exosome-based therapies in regenerative medicine and neurodegenerative diseases.

## **Materials and Methods**

### **Culture and characterization of UC-MSCs**

UC-MSCs at passage 3 were obtained frozen in liquid nitrogen from the biobank of Mashhad University of Medical Sciences. The cells were thawed by placing the vial in a 37°C water bath

for 1 min, and the contents of the vial were immediately transferred to T75 flasks containing alpha-minimum essential medium (Gibco, USA) culture medium supplemented with 10% fetal bovine serum (FBS; Gibco, USA), 1% penicillin/streptomycin (Sigma-Aldrich, USA), and 1% L-glutamine (Gibco, USA). The total volume of culture medium in each flask was limited to a maximum of 10 mL, and the cells were maintained in an incubator at 37°C, 95% humidity, and 5% CO<sub>2</sub>. The cell culture medium was changed every 48 to 72 h. Before cell passage, flow cytometry was performed on mesenchymal cells to characterize positive (CD90, CD44) and negative (CD45, CD11b) markers. For assessing the expression of these positive and negative markers, approximately  $1 \times 10^6$  UC-MSCs were collected and washed with cold phosphate-buffered saline (PBS) to remove any residual culture medium. The cells were then resuspended in PBS containing 2% FBS and maintained at 4°C. To reduce non-specific binding, they were blocked in PBS with 5% FBS for 15 minutes at 4°C. Following the blocking step, the cells were incubated in a final volume of 100  $\mu$ L with fluorophore-conjugated antibodies targeting CD90, CD44, CD45, and CD11b (BD Biosciences, USA) for 30 minutes at 4°C in the dark. After incubation, the cells were washed twice with PBS containing 2% FBS to remove any unbound antibodies. Finally, the cells were resuspended in PBS with 2% FBS and at least 10,000 events per sample were recorded using a flow cytometer (BD FACSCanto II). The data were then analyzed with FlowJo software, with gating established using unstained controls. After reaching 80–90% confluence, cells were detached from the bottom of the flask with 0.25% trypsin-EDTA (Gibco, USA) (for 1–3 min) and neutralized by adding medium (for passage). After reaching >80% confluence at passage 4, the cell culture medium was replaced with FBS-free medium (48 h before the exosome extraction process began), and cell compliance was assessed for spindle

morphology and adhesion within 24–48 h. Cell viability was confirmed by trypan blue (Gibco, USA) exclusion ( $\geq 95\%$ ).

### **Exosome isolation**

After the cells were prepared to start the exosome isolation process, the supernatant from the cells was poured into 5 sterile falcons (14 ml per falcon, total 70 ml) and subjected to sequential centrifugation steps to remove cellular debris. This process included centrifugation cycles of  $2000\times g$  for 10 min,  $5000\times g$  for 20 min, and  $10000\times g$  for 30 min (fixed-angle rotor), all performed at  $4^{\circ}\text{C}$ . In this process, exosomes and other small particles such as microvesicles ( $\sim 100\text{--}1000$  nm) remain floating in the medium, and the debris is closer to the bottom of the falcons. Accordingly, after each centrifugation, the medium at the bottom of the falcons (2 ml per falcon) was discarded and the upper medium was transferred to new falcons. After completing the centrifugation steps, the remaining supernatant (40 ml) was passed through a 0.22-micron syringe filter (Millipore, USA) to remove residual particles and possible contaminants. Then, the supernatant was poured into five sterile ultracentrifuge falcons (8 ml each). For the final separation of exosomes and their concentration, the sample was subjected to two consecutive ultracentrifuges at  $100,000\times g$  for 70 minutes at  $4^{\circ}\text{C}$  to sediment the exosomes at the bottom of the falcons in a Beckman Coulter Optima (fixed-angle rotor). After the first time, the supernatant was completely removed and an equal volume of sterile PBS was added to the falcons and they were subjected to ultracentrifugation for a second time. Finally, all PBS in the falcons was removed, and the exosome pellet was washed by adding sterile and filtered PBS (with a 0.22-micron syringe filter) again in an amount of  $300\text{ }\mu\text{l}$  per falcon (total 1.5 ml) and used for the continuation of the research processes.

## **Exosome Characterization**

### **BCA assay**

The total protein content of exosomes was measured using a BCA protein concentration determination kit (Pars Toos, Iran) and according to the manufacturer's protocol. In this method, exosomal samples were mixed in a 96-well microplate with BCA reagent and incubated for 60 minutes at 37°C. Finally, the optical absorbance at a wavelength of 562 nm was measured using a NanoDrop 2000 spectrophotometer (Thermo Fisher Scientific, USA), and the total protein concentration was calculated based on the standard curve.

### **TEM analysis**

Exosomes were fixed in 2% paraformaldehyde solution (Merck, Germany), adsorbed onto Formvar-carbon-coated grids, and negatively stained with 2% uranyl acetate (Electron Microscopy Sciences, USA). Their morphology and size were examined using a JEOL JEM-1400 Flash transmission electron microscope (JEOL, Japan) at 80 kV.

### **DLS measurements**

Size distribution and zeta potential were measured using a Horiba Scientific SZ-100 nanoparticle analyzer (Horiba Ltd., Kyoto, Japan). Samples were diluted 1:100 in PBS and analyzed at 25°C. A summary of the steps of isolation and characterization of exosomes in the present study is shown in Figure 1.



## **Western blot analysis**

Exosomal protein and UC-MSC whole-cell lysate protein were mixed with 4× Laemmli sample buffer, boiled for 5 min, and loaded onto 10% SDS–PAGE gels. Proteins were separated at 120 V for 90 min and transferred onto polyvinylidene difluoride (PVDF) membranes (Immobilon-P, Millipore) at 100 V for 1 h in transfer buffer (25 mM Tris, 192 mM glycine, 20% methanol). Membranes were blocked with 5% non-fat dry milk in TBST (0.1% Tween-20 in Tris-buffered saline) for 1 h at room temperature. Blots were then incubated overnight at 4 °C with the following primary antibodies diluted in blocking buffer: anti-CD9 (1:1,000; Abcam, ab92726), anti-CD63 (1:1,000; Abcam, ab8219), and anti-calnexin (1:2,000; Cell Signaling Technology, #2679). After three washes in TBST (5 min each), membranes were incubated for 1 h at room temperature with HRP-conjugated secondary antibodies (anti-mouse IgG–HRP or anti-rabbit IgG–HRP, 1:5,000; Invitrogen). Following three additional TBST washes, bands were visualized by enhanced chemiluminescence (ECL Western Blotting Substrate, Thermo Fisher) and imaged using a gel documentation system (Bio-Rad ChemiDoc).

## **Results**

### **Morphological Progression of UC-MSCs**

At the passage 3, mesenchymal cells derived from umbilical cord exhibited a distinct fibroblastic morphology and exhibited strong adherence to the substrate. As the density of the cells increased, it became evident that subculturing was necessary. Following the process of reseeding, the initial passage of four cultures demonstrated a uniform cell distribution, indicative of successful proliferation. By the end of passage 4, the cultures attained approximately 80% confluence. At this stage, the cells were transferred to a medium devoid of FBS to prevent

contamination from serum-derived vesicles and to improve both the yield and purity of the exosomes that were subsequently isolated (Figure 2).

### **Characterization of surface markers of UC-MSCs using flow cytometry**

Flow cytometry analysis was performed to investigate the surface characteristics of UC-MSCs. The results showed that the cells had high expression of mesenchymal-specific markers, such as CD90 and CD44, while the hematopoietic markers CD45 and CD11b were not expressed. These results were confirmed by flow cytometry images and indicate the mesenchymal nature of the cells (Figure 3).

### **Exosomal protein quantification using the BCA assay**

Conditioned media from seven identical T75 flasks were pooled prior to exosome isolation. Based on the linear regression equation ( $R^2 = 0.9908$ ), the total protein concentration of the pooled exosome sample was approximately 7687.5  $\mu\text{g/mL}$ , corresponding to an average yield of about 1098.2  $\mu\text{g/mL}$  per T75 flask. This concentration provided a sufficient amount of exosomal protein for downstream functional experiments.

### **Morphological characterization of exosomes using TEM**

TEM images revealed a spherical or cup-shaped morphology and a distinct bilayer membrane in the extracted exosomes. The dimensions of the exosomes were in the range of 30–150 nm, which is consistent with the expected sizes for these extracellular vesicles. The images confirm the characteristic structure and intact membrane of the exosomes, indicating the high purity of the extracted samples (Figure 4).

### **Determination of size and zeta potential of exosomes by DLS**

DLS offered three complementary perspectives on the size distribution of exosomes (Figure 5). The number-weighted distribution (Figure 5, A) identified a prominent peak at  $121.3 \pm 23.7$  nm, signifying the most prevalent particle size by count. The volume-weighted distribution (Figure 5, B) supported this observation, indicating that particles of this size constitute the largest portion of the total sample volume. The intensity-weighted distribution (Figure 5, C) further validated the presence of a monodisperse population, with a polydispersity index (PDI) below 0.3, reflecting high uniformity and minimal aggregation. These DLS profiles confirm the consistency and appropriateness of the isolated exosomes for subsequent functional assays. Zeta-potential assessments were conducted in two separate replicates to evaluate the surface charge and colloidal stability of the isolated exosomes (Figure 6). The initial analysis (Figure 6, A) revealed that the exosomes had a mean zeta potential of  $-37.3$  mV, indicating a stable population of negatively charged vesicles. The confirmatory replicate (Figure 6, B) produced a highly consistent mean value of  $-43.8$  mV. Collectively, these findings illustrate a reproducible negative surface charge, which is associated with a low tendency for aggregation and appropriateness for subsequent functional assays.

### **Western blot validation of exosomal markers**

As shown in Figure 7, CD9 and CD63 were readily detected in both exosome replicates, while calnexin was absent from exosomal lanes and present only in the UC-MSC cell lysate. This confirms successful enrichment of vesicular markers and negligible endoplasmic reticulum contamination, fulfilling MISEV guidelines for protein marker validation.

## Discussion

The present study aimed to design a standard protocol based on the MISEV guidelines for isolating and characterizing therapeutic-grade exosomes from UC-MSCs. Our study offers a robust and reproducible approach for isolating exosomes from UC-MSCs, combining differential centrifugation and ultracentrifugation with advanced characterization techniques including TEM, DLS, and BCA. This integrated strategy effectively overcomes common limitations such as low purity and compromised vesicle integrity, while highlighting the favorable physicochemical properties and therapeutic relevance of the isolated exosomes—an important step toward their clinical application.

A common challenge in studies of stem cell-derived exosomes is the heterogeneity of cell sources (Hassanzadeh et al., 2021). To ensure the quality, safety, and efficacy of cell-based therapies, the International Society for Cell and Gene Therapy (ISCT) deems it necessary to confirm cell purity based on specific markers (Guadix et al., 2019). In our study, UC-MSCs were characterized by flow cytometry, which confirmed their mesenchymal identity through the presence of CD90 and CD44, and the absence of hematopoietic markers CD45 and CD11b. Furthermore, standardizing exosome studies requires the use of well-defined, contamination-free culture conditions (Abramowicz et al., 2018; Wang, Tsai, & Lee, 2024). To reduce the risk of exogenous vesicle contamination, this study employed FBS-free culture media prior to exosome isolation. These findings align with recent studies that highlight the importance of quality control in MSC preparation (Krishnan et al., 2025; Wang et al., 2024).

In the next step, TEM and DLS were used to confirm the quality of the isolated exosomes in terms of morphology, size distribution, and colloidal stability. Following established standards, the simultaneous use of TEM and DLS as two complementary methods allowed for a more

detailed analysis of the physical properties of the sample (Rupert, Claudio, Lässer, & Bally, 2017). TEM provided high-resolution morphological details, while DLS confirmed the particle size distribution in the dispersing medium and minimized the risk of particle aggregation for potential therapeutic applications (Khodabandehloo & Chen, 2017). Using the differential centrifugation and ultracentrifugation protocol made the efficient isolation of samples possible without damaging their structure, which played a key role in reducing errors caused by sample heterogeneity. These findings are consistent with previous studies (Ishii, Noguchi, Ikemoto, Yohda, & Odahara, 2023; Muller, Hong, Stolz, Watkins, & Whiteside, 2014; Patel et al., 2019; Tieu et al., 2020). In the context of the MISEV guidelines, Ishii et al. have emphasized that the combination of imaging methods, such as TEM, and dynamic analysis, like DLS, is essential to confirm the morphological uniformity and size distribution of exosomes (Ishii et al., 2023). Similarly, Muller et al. in a study on plasma-derived exosomes showed that the simultaneous use of ultracentrifugation and differential centrifugation increases the isolation efficiency without destroying the vesicle structure (Muller et al., 2014). Furthermore, Tieu et al. in a systematic review noted that differential centrifugation-ultracentrifugation-based protocols, despite their simplicity, can produce samples of sufficient purity for functional studies, especially when used in conjunction with TEM/DLS confirmations (Tieu et al., 2020). Patel et al. observed a significant reduction in particle aggregation in samples processed by ultracentrifuge and concluded that this was likely due to the preservation of colloidal stability during the isolation process (Patel et al., 2019). This convergence across different studies supports the validity of the present methodology and points to the importance of using multiple analytical standards in exosome characterization. Moreover, Western blot analysis confirmed robust detection of canonical exosomal markers CD9 and CD63 in both vesicle replicates, while calnexin was

undetectable in these fractions, demonstrating negligible endoplasmic reticulum contamination. This orthogonal protein-based validation complements our TEM and DLS characterizations, fully satisfying MISEV criteria and reinforcing the purity and reproducibility of the UC-MSC exosome isolation protocol.

The use of the BCA revealed a high protein concentration of exosomes, which is sufficient for functional studies. However, recent studies have shown that the typical protein concentration of exosomes extracted by standard methods such as ultracentrifugation and SEC is below or approximately equal to 1000  $\mu\text{g/mL}$  (Alameldin et al., 2021; Bok et al., 2024; Guan et al., 2020). The most important reason for these differences may lie in variations in cell number (or final cell flasks and their volume) and supernatant pooling, which linearly increases the number of exosomes and associated proteins, especially if the final extraction volume is small (Ferguson & Nguyen, 2016; Théry, Amigorena, Raposo, & Clayton, 2006). However, accurate identification of protein content requires more advanced proteomic analyses, such as mass spectrometry, to ensure the absence of contaminants like apolipoproteins or albumin (Yi et al., 2024). This is especially critical in studies aimed at the therapeutic use of exosomes, as the presence of impurities can affect their efficacy and/or safety.

Despite the strengths of this protocol, some limitations should be taken into consideration. This protocol is effective for research purposes, but scaling up production for clinical applications is challenging, as ultracentrifugation methods rely on expensive and time-consuming equipment (Ansari et al., 2024). Although the physical and biochemical properties of exosomes have been characterized, the lack of functional data in specific disease models, such as neurodegenerative disorders, is a limitation, and future studies should evaluate the efficacy of these exosomes in modulating inflammation or tissue repair. This study did not provide an in-depth analysis of the

molecular cargo of exosomes (such as miRNAs, proteins, and lipids), as detailed knowledge of these components is essential for the design of targeted therapies. This study focuses exclusively on UC-MSCs, and comparisons with exosomes derived from other MSC sources, such as bone marrow or adipose tissue, are crucial to identify the most suitable source for specific applications. The transfer of exosomes to the clinical stage requires compliance with stringent regulatory requirements that were not addressed in this study, and standardization of manufacturing processes and safety assessment are key challenges. To improve this protocol and accelerate the clinical translation of exosomes, exploring alternative methods such as tangential flow filtration or the use of bioreactors could increase production yields without compromising quality (Ma et al., 2024).

## **Conclusions**

This study provides a standardized protocol for the isolation and characterization of therapeutic-grade exosomes from UC-MSCs that addresses key challenges in purity, reproducibility, and identification. The high-concentration exosomes produced by this method have significant potential for advancing regenerative medicine and treating neurodegenerative diseases, providing a solid foundation for translational research. However, to fully assess their clinical potential, further improvement is needed in areas such as scalability, functional validation, and compliance with regulatory standards.

## **Data availability statement**

The data that support the findings of this study are available from the corresponding author if requested.

### **Ethics approval statement**

This project was approved by the Ethics Committee of Mashhad University of Medical Sciences, Mashhad, Iran (Code: IR.MUMS.AEC.1402.004).

### **Acknowledgments**

We extend our appreciation to the technical and administrative staff of Department of Neuroscience, Mashhad University of Medical Sciences for their invaluable assistance. Special thanks to colleagues and collaborators for their insightful feedback and contributions to this work.

### **Funding**

This article was taken from the PhD dissertation of Amir Bavafa (Tracking code: 4012020), approved by Department of Neuroscience, Faculty of Medicine, Mashhad University of Medical Sciences, Mashhad, Iran. This study was financially supported by Mashhad University of Medical Sciences, Mashhad, Iran.

### **Authors' contributions**

Conceptualization: A.B; Methodology: A.B, A.S and S.S-N; Investigation and resources: A.B and A.S; Writing the original draft, and funding acquisition: A.B; Review, and editing: A.S, S.S-N, F.F and A.G; Supervision: A.S, S.S-N and A.G.

### **Declarations of interest**

The authors declared no conflict of interest.



## References

- Abramowicz, A., Marczak, L., Wojakowska, A., Zapotoczny, S., Whiteside, T. L., Widlak, P., & Pietrowska, M. (2018). Harmonization of exosome isolation from culture supernatants for optimized proteomics analysis. *PloS one*, 13(10), e0205496.
- Akbar, A., Malekian, F., Baghban, N., Kodam, S. P., & Ullah, M. (2022). Methodologies to isolate and purify clinical grade extracellular vesicles for medical applications. *Cells*, 11(2), 186.
- Alameldin, S., Costina, V., Abdel-Baset, H. A., Nitschke, K., Nuhn, P., Neumaier, M., & Hedtke, M. (2021). Coupling size exclusion chromatography to ultracentrifugation improves detection of exosomal proteins from human plasma by LC-MS. *Practical Laboratory Medicine*, 26, e00241.
- Ansari, F. J., Tafti, H. A., Amanzadeh, A., Rabbani, S., Shokrgozar, M. A., Heidari, R., . . . Ghanbari, H. (2024). Comparison of the efficiency of ultrafiltration, precipitation, and ultracentrifugation methods for exosome isolation. *Biochemistry and biophysics reports*, 38, 101668.
- Bai, L., Yu, L., Ran, M., Zhong, X., Sun, M., Xu, M., . . . Tang, Y. (2025). Harnessing the Potential of Exosomes in Therapeutic Interventions for Brain Disorders. *International Journal of Molecular Sciences*, 26(6), 2491.
- Bok, E.-Y., Seo, S. Y., Lee, H. G., Wimalasena, S. H. M. P., Kim, E., Cho, A., . . . Lee, S.-L. (2024). Exosomes isolation from bovine serum: Qualitative and quantitative comparison between ultracentrifugation, combination ultracentrifugation and size exclusion chromatography, and exoEasy methods. *Journal of Animal Science and Technology*, 66(5), 1021.
- Chen, J., Li, P., Zhang, T., Xu, Z., Huang, X., Wang, R., & Du, L. (2022). Review on strategies and technologies for exosome isolation and purification. *Frontiers in bioengineering and biotechnology*, 9, 811971.
- Cui, E., Lv, L., Wang, B., Li, L., Lu, H., Hua, F., . . . Pan, R. (2024). Umbilical cord MSC-derived exosomes improve alveolar macrophage function and reduce LPS-induced acute lung injury. *Journal of Cellular Biochemistry*, 125(2), e30519.
- Ferguson, S. W., & Nguyen, J. (2016). Exosomes as therapeutics: the implications of molecular composition and exosomal heterogeneity. *Journal of Controlled Release*, 228, 179-190.
- Guadix, J. A., López-Beas, J., Clares, B., Soriano-Ruiz, J. L., Zugaza, J. L., & Gálvez-Martín, P. (2019). Principal criteria for evaluating the quality, safety and efficacy of hMSC-based products in clinical practice: current approaches and challenges. *Pharmaceutics*, 11(11), 552.
- Guan, S., Yu, H., Yan, G., Gao, M., Sun, W., & Zhang, X. (2020). Characterization of urinary exosomes purified with size exclusion chromatography and ultracentrifugation. *Journal of proteome research*, 19(6), 2217-2225.
- Hassanzadeh, A., Rahman, H. S., Markov, A., Endjun, J. J., Zekiy, A. O., Chartrand, M. S., . . . Nikoo, M. (2021). Mesenchymal stem/stromal cell-derived exosomes in regenerative medicine and cancer; overview of development, challenges, and opportunities. *Stem cell research & therapy*, 12(1), 297.
- Hussen, B. M., Taheri, M., Yashooa, R. K., Abdullah, G. H., Abdullah, S. R., Kheder, R. K., & Mustafa, S. A. (2024). Revolutionizing medicine: recent developments and future prospects in stem-cell therapy. *International Journal of Surgery*, 110(12), 8002-8024.

Ishii, N., Noguchi, K., Ikemoto, M. J., Yohda, M., & Odahara, T. (2023). Optimizing exosome preparation based on size and morphology: Insights from electron microscopy. *Microscopy and Microanalysis*, 29(6), 2068-2079.

Jia, Y., Yu, L., Ma, T., Xu, W., Qian, H., Sun, Y., & Shi, H. (2022). Small extracellular vesicles isolation and separation: Current techniques, pending questions and clinical applications. *Theranostics*, 12(15), 6548.

Jiao, Y., Yang, L., Wang, R., Song, G., Fu, J., Wang, J., . . . Wang, H. (2024). Drug Delivery Across the Blood–Brain Barrier: A New Strategy for the Treatment of Neurological Diseases. *Pharmaceutics*, 16(12), 1611.

Jin, H. J., Bae, Y. K., Kim, M., Kwon, S.-J., Jeon, H. B., Choi, S. J., . . . Chang, J. W. (2013). Comparative analysis of human mesenchymal stem cells from bone marrow, adipose tissue, and umbilical cord blood as sources of cell therapy. *International Journal of Molecular Sciences*, 14(9), 17986-18001.

Kang, J., & Guo, Y. (2022). Human umbilical cord mesenchymal stem cells derived exosomes promote neurological function recovery in a rat spinal cord injury model. *Neurochemical Research*, 47(6), 1532-1540.

Khodabandehloo, A., & Chen, D. D. Y. (2017). Particle sizing methods for the detection of protein aggregates in biopharmaceuticals. *Bioanalysis*, 9(3), 313-326.

Krishnan, I., Ng, C. Y., Kee, L. T., Ng, M. H., Law, J. X., Thangarajah, T., . . . Subramani, B. (2025). Quality Control of Fetal Wharton's Jelly Mesenchymal Stem Cells-Derived Small Extracellular Vesicles. *International Journal of Nanomedicine*, 1807-1820.

Lee, K. W. A., Chan, L. K. W., Hung, L. C., Phoebe, L. K. W., Park, Y., & Yi, K.-H. (2024). Clinical applications of exosomes: a critical review. *International Journal of Molecular Sciences*, 25(14), 7794.

Li, T., Xia, M., Gao, Y., Chen, Y., & Xu, Y. (2015). Human umbilical cord mesenchymal stem cells: an overview of their potential in cell-based therapy. *Expert opinion on biological therapy*, 15(9), 1293-1306.

Luan, Z., Liu, J., Li, M., Wang, Y., & Wang, Y. (2024). Exosomes derived from umbilical cord-mesenchymal stem cells inhibit the NF- $\kappa$ B/MAPK signaling pathway and reduce the inflammatory response to promote recovery from spinal cord injury. *Journal of orthopaedic surgery and research*, 19(1), 184.

Ma, Y., Dong, S., Grippin, A. J., Teng, L., Lee, A. S., Kim, B. Y., & Jiang, W. (2024). Engineering therapeutical extracellular vesicles for clinical translation. *Trends in Biotechnology*.

Miron, R. J., & Zhang, Y. (2024). Understanding exosomes: Part 1—Characterization, quantification and isolation techniques. *Periodontology 2000*, 94(1), 231-256.

Muller, L., Hong, C.-S., Stolz, D. B., Watkins, S. C., & Whiteside, T. L. (2014). Isolation of biologically-active exosomes from human plasma. *Journal of immunological methods*, 411, 55-65.

Nouri, Z., Barfar, A., Perseh, S., Motasadizadeh, H., Maghsoudian, S., Fatahi, Y., . . . Atyabi, F. (2024). Exosomes as therapeutic and drug delivery vehicle for neurodegenerative diseases. *Journal of Nanobiotechnology*, 22(1), 463.

Patel, G. K., Khan, M. A., Zubair, H., Srivastava, S. K., Khushman, M. d., Singh, S., & Singh, A. P. (2019). Comparative analysis of exosome isolation methods using culture supernatant for optimum yield, purity and downstream applications. *Scientific reports*, 9(1), 5335.

Rupert, D. L., Claudio, V., Lässer, C., & Bally, M. (2017). Methods for the physical characterization and quantification of extracellular vesicles in biological samples. *Biochimica et Biophysica Acta (BBA)-General Subjects*, 1861(1), 3164-3179.

Théry, C., Amigorena, S., Raposo, G., & Clayton, A. (2006). Isolation and characterization of exosomes from cell culture supernatants and biological fluids. *Current protocols in cell biology*, 30(1), 3.22. 21-23.22. 29.

Théry, C., Witwer, K. W., Aikawa, E., Alcaraz, M. J., Anderson, J. D., Andriantsitohaina, R., . . . Atkin-Smith, G. K. (2018). Minimal information for studies of extracellular vesicles 2018 (MISEV2018): a position statement of the International Society for Extracellular Vesicles and update of the MISEV2014 guidelines. *Journal of extracellular vesicles*, 7(1), 1535750.

Tieu, A., Lalu, M. M., Slobodian, M., Gnyra, C., Fergusson, D. A., Montroy, J., . . . Allan, D. S. (2020). An analysis of mesenchymal stem cell-derived extracellular vesicles for preclinical use. *ACS nano*, 14(8), 9728-9743.

Wang, C. K., Tsai, T. H., & Lee, C. H. (2024). Regulation of exosomes as biologic medicines: Regulatory challenges faced in exosome development and manufacturing processes. *Clinical and Translational Science*, 17(8), e13904.

Welsh, J. A., Goberdhan, D. C., O'Driscoll, L., Buzas, E. I., Blenkiron, C., Bussolati, B., . . . Erdbrügger, U. (2024). Minimal information for studies of extracellular vesicles (MISEV2023): From basic to advanced approaches. *Journal of extracellular vesicles*, 13(2), e12404.

Xiong, M., Chen, Z., Tian, J., Peng, Y., Song, D., Zhang, L., & Jin, Y. (2024). Exosomes derived from programmed cell death: mechanism and biological significance. *Cell Communication and Signaling*, 22(1), 156.

Yadav, A., Xuan, Y., Sen, C. K., & Ghatak, S. (2024). Standardized reporting of research on exosomes to ensure rigor and reproducibility. *Advances in Wound Care*, 13(11), 584-599.

Yadav, K., Vijayalakshmi, R., Sahu, K. K., Sure, P., Chahal, K., Yadav, R., . . . Pradhan, M. (2024). Exosome-based macromolecular neurotherapeutic drug delivery approaches in overcoming the blood-brain barrier for treating brain disorders. *European Journal of Pharmaceutics and Biopharmaceutics*, 114298.

Yi, G., Luo, H., Zheng, Y., Liu, W., Wang, D., & Zhang, Y. (2024). Exosomal proteomics: unveiling novel insights into lung cancer. *Aging Dis*.

Yin, H., You, S., Li, X., Li, S., & Guo, C. (2024). Progress, challenges, and prospects of small extracellular vesicles isolation and characterization. *Journal of Holistic Integrative Pharmacy*, 5(2), 121-130.

Zhang, Y., Lan, M., & Chen, Y. (2024). Minimal Information for Studies of Extracellular Vesicles (MISEV): Ten-Year Evolution (2014–2023). *Pharmaceutics*, 16(11), 1394.

## Tables/Figure Legends

**Figure 1.** From cell culture to exosome characterization

**Figure 2.** Morphology of umbilical-cord-derived mesenchymal cells through successive passages. (A) Cells at the end of passage 3, exhibiting typical fibroblastic morphology and firm adhesion. (B) Cells immediately prior to subculture, illustrating increased density and the necessity for passaging. (C) Early passage 4, showing a uniform distribution of cells following replating. (D) Approximately 80 % confluence at the end of passage 4, indicating readiness for transfer into FBS-free medium for exosome isolation.

**Figure 3.** Phenotypic characterization of UC-MSCs. (A) shows the expression of the UC-MSC surface marker CD90-PE (FL-2), (B) displays CD44-PerCp expression (FL-3), (C) indicates the absence of expression for CD45-FITC (FL-1), (D) indicates the absence of expression for CD11b-APC (FL-4).

**Figure 4.** TEM images confirming the classical morphology of exosomes; Scale bar: 100 nm

**Figure 5.** DLS analysis of UC-MSC-derived exosomes. (A) Number-weighted size distribution, highlighting the predominant particle diameter. (B) Volume-weighted size distribution, showing the relative volume contribution across size classes. (C) Intensity-weighted size distribution, reflecting the relative scattering intensity and confirming sample monodispersity.

**Figure 6.** Zeta-potential analysis of UC-MSC-derived exosomes (two independent replicates).

**Figure 7.** Western blot analysis of exosomal and cellular markers; Lane 1 (left side) corresponds to the whole cell lysate (Cell), and lanes 2 (middle) and 3 (right side) represent two technical

replicates of exosomes (Exosomes 1 and Exosomes 2) isolated from the same batch of UC-MSC-conditioned medium.

## Tables and Figures

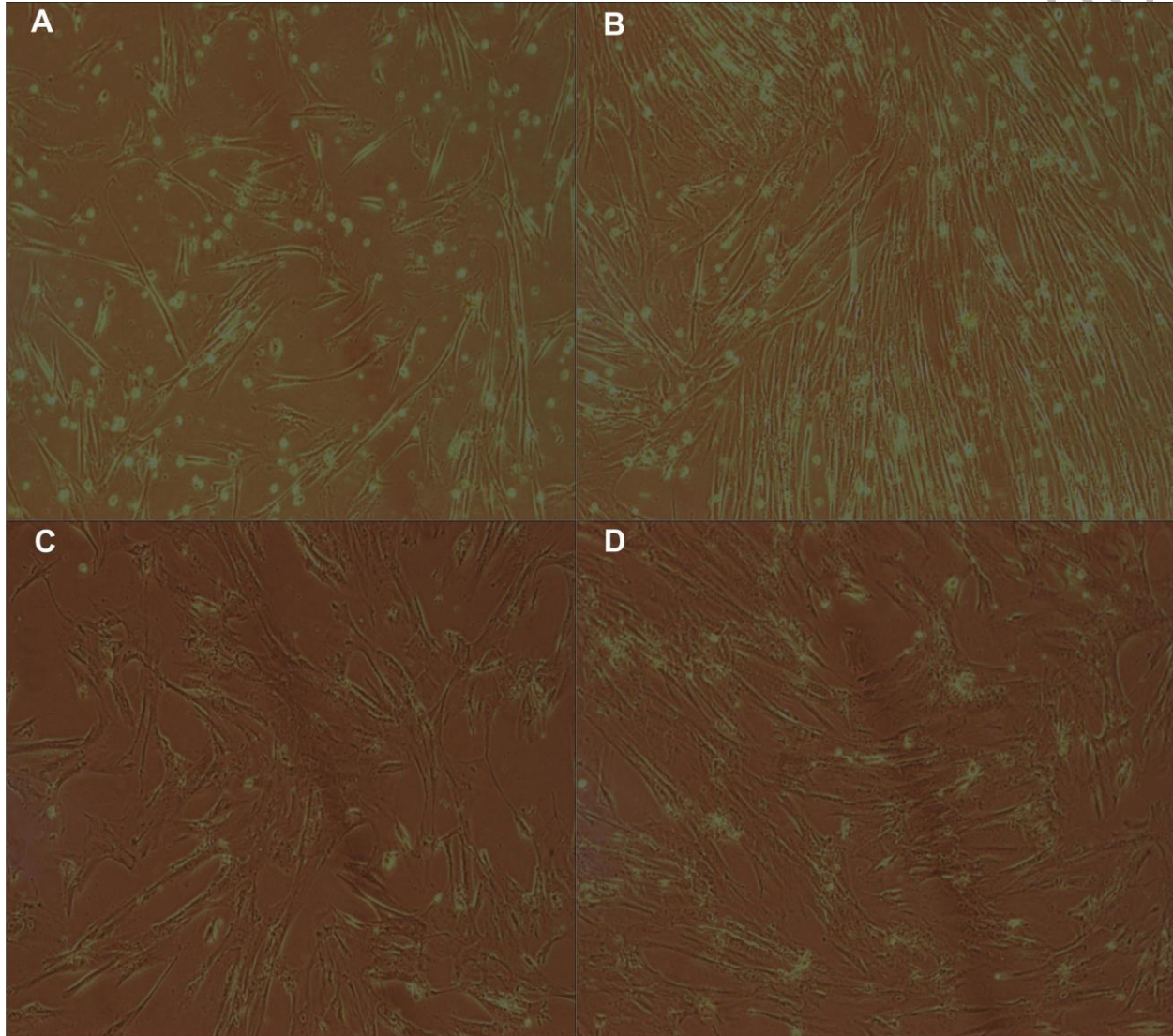


**Figure 2.** Morphology of umbilical-cord-derived mesenchymal cells through successive passages. (A) Cells at the end of passage 3, exhibiting typical fibroblastic morphology and firm adhesion. (B) Cells immediately prior to subculture, illustrating increased density and the necessity for passaging. (C) Early passage 4, showing a uniform distribution of cells following replating. (D) Approximately 80 % confluence at the end of passage 4, indicating readiness for transfer into FBS-free medium for exosome isolation.

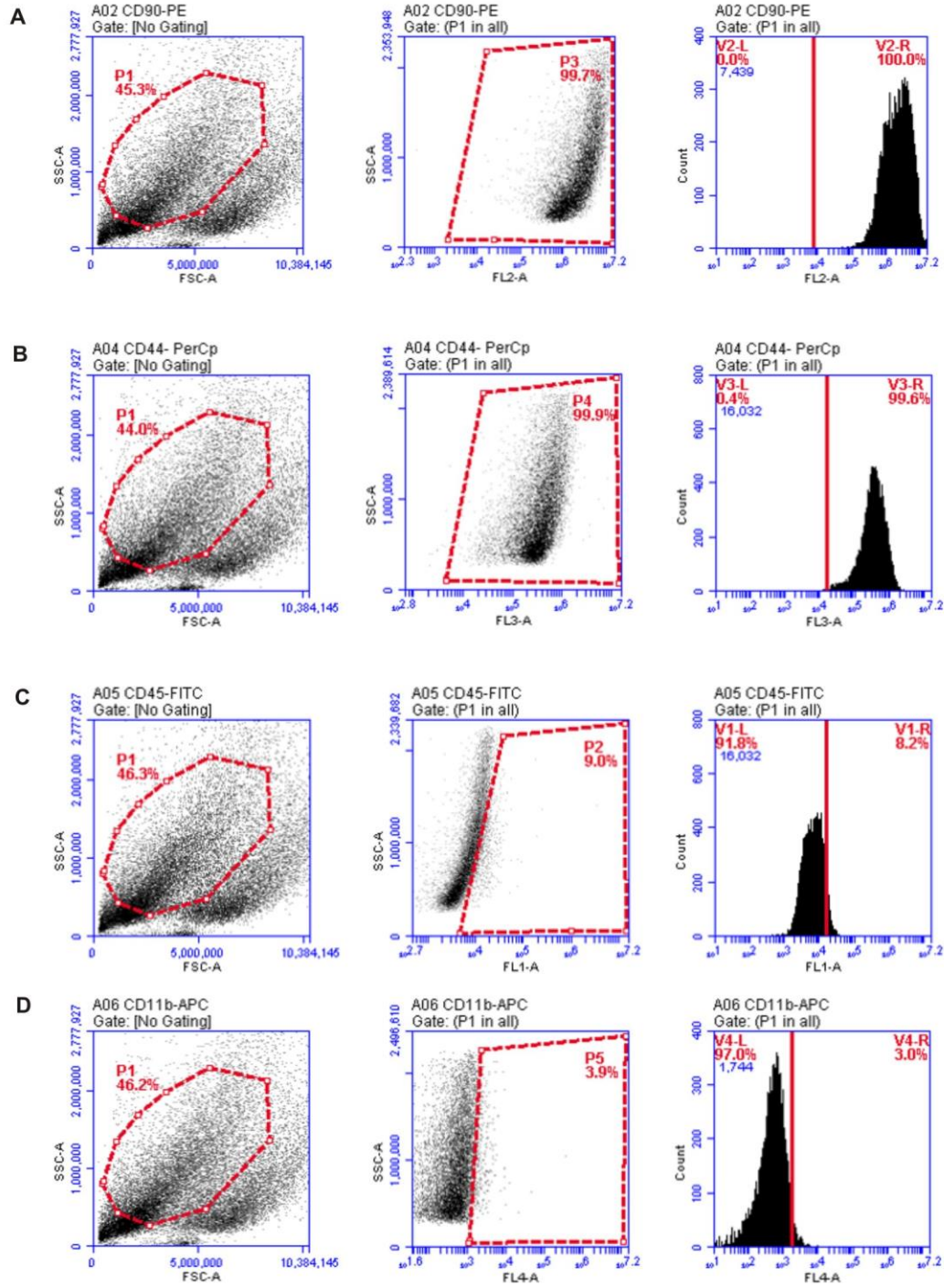


**Figure 3.** Phenotypic characterization of UC-MSCs. (A) shows the expression of the UC-MSC surface marker CD90-PE (FL-2), (B) displays CD44-PerCp expression (FL-3), (C) indicates the absence of expression for CD45-FITC (FL-1), (D) indicates the absence of expression for CD11b-APC (FL-4).



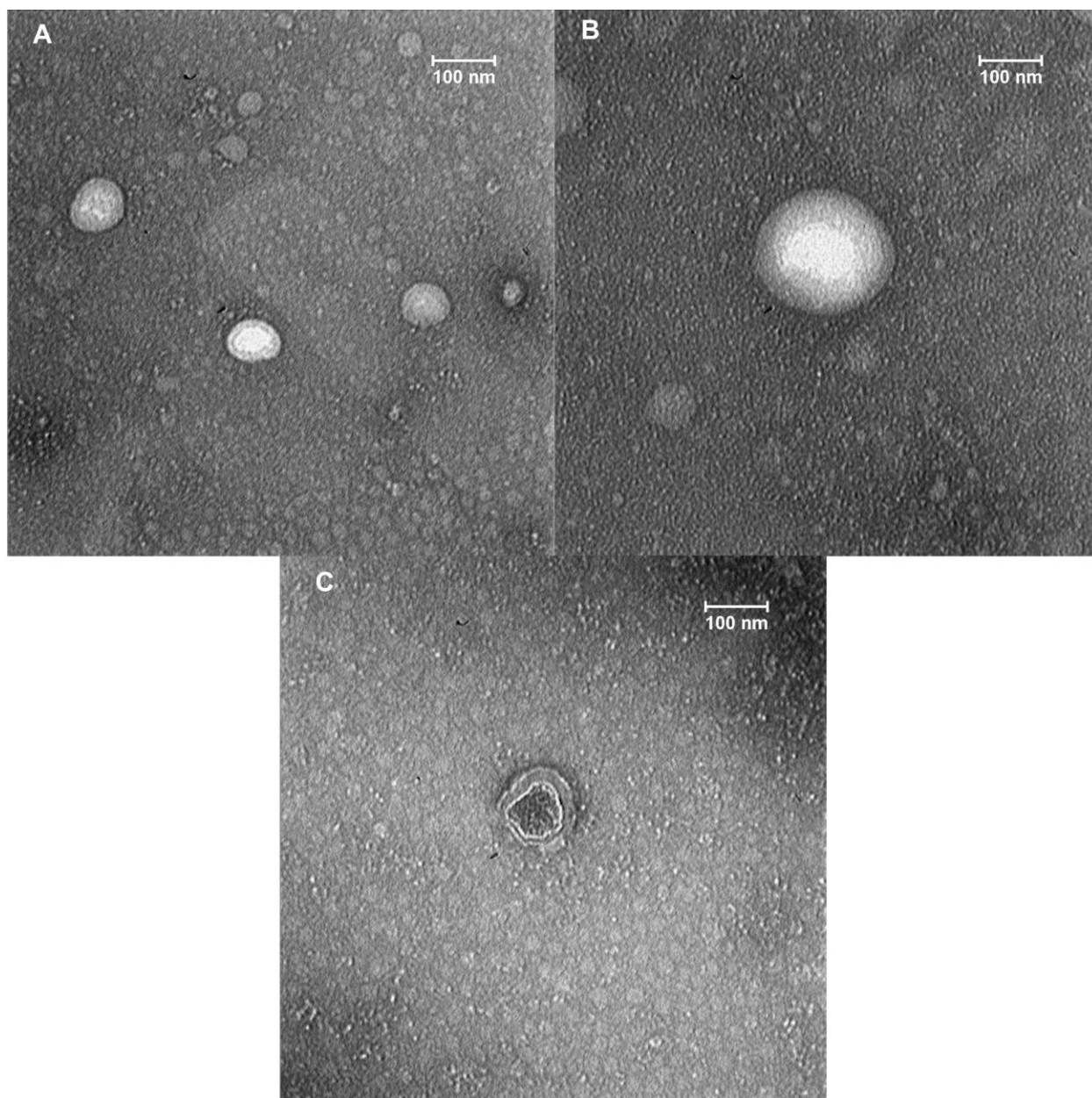


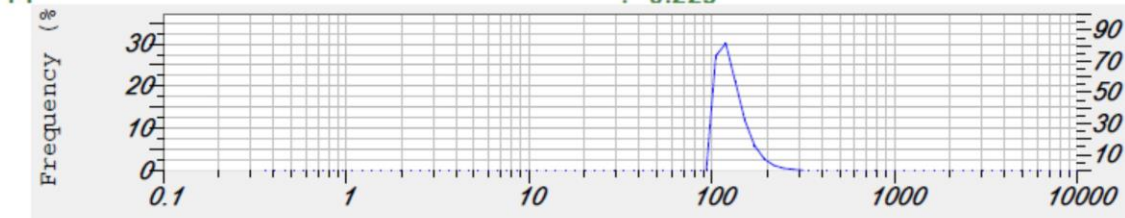
**Figure 4.** TEM images confirming the classical morphology of exosomes; Scale bar: 100 nm

## A Calculation Results

Peak No.	S.P.Area Ratio	Mean	S. D.	Mode
1	1.00	121.3 nm	23.7 nm	110.3 nm
2	---	--- nm	--- nm	--- nm
3	---	--- nm	--- nm	--- nm
Total	1.00	121.3 nm	23.7 nm	110.3 nm

### Cumulant Operations

Z-Average : 169.0 nm  
PI : 0.229

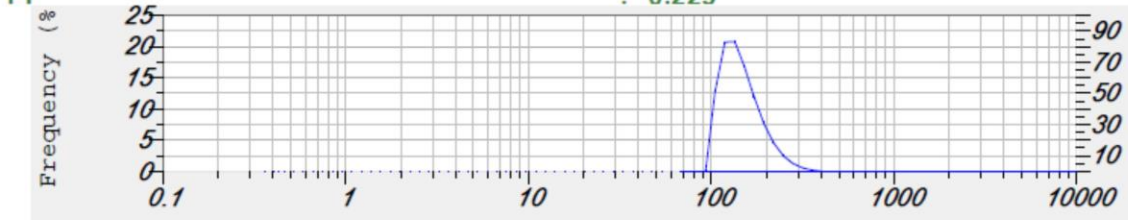


## B Calculation Results

Peak No.	S.P.Area Ratio	Mean	S. D.	Mode
1	1.00	140.1 nm	37.3 nm	124.8 nm
2	---	--- nm	--- nm	--- nm
3	---	--- nm	--- nm	--- nm
Total	1.00	140.1 nm	37.3 nm	124.8 nm

### Cumulant Operations

Z-Average : 169.0 nm  
PI : 0.229



## C Calculation Results

Peak No.	S.P.Area Ratio	Mean	S. D.	Mode
1	1.00	177.7 nm	55.3 nm	160.7 nm
2	---	--- nm	--- nm	--- nm
3	---	--- nm	--- nm	--- nm
Total	1.00	177.7 nm	55.3 nm	160.7 nm

### Cumulant Operations

Z-Average : 169.0 nm  
PI : 0.229

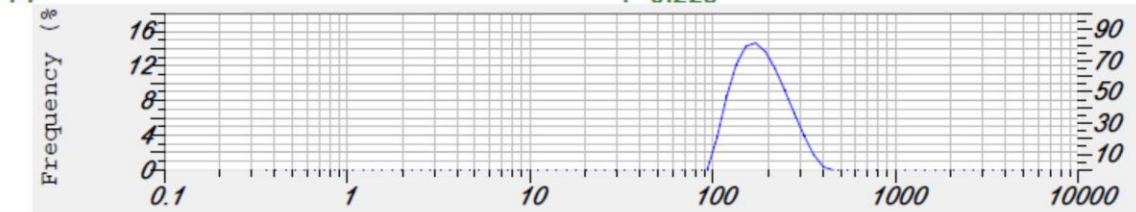


**Figure 5.** DLS analysis of UC-MSC-derived exosomes. (A) Number-weighted size distribution, highlighting the predominant particle diameter. (B) Volume-weighted size distribution, showing the relative volume contribution across size classes. (C) Intensity-weighted size distribution, reflecting the relative scattering intensity and confirming sample monodispersity.



**A**

### Calculation Results

Peak No.	Zeta Potential	Electrophoretic Mobility
1	-37.3 mV	-0.000289 cm <sup>2</sup> /Vs
2	--- mV	--- cm <sup>2</sup> /Vs
3	--- mV	--- cm <sup>2</sup> /Vs

Zeta Potential (Mean) : -37.3 mV  
Electrophoretic Mobility Mean : -0.000289 cm<sup>2</sup>/Vs

**B**

### Calculation Results

Peak No.	Zeta Potential	Electrophoretic Mobility
1	-43.8 mV	-0.000340 cm <sup>2</sup> /Vs
2	--- mV	--- cm <sup>2</sup> /Vs
3	--- mV	--- cm <sup>2</sup> /Vs

Zeta Potential (Mean) : -43.8 mV  
Electrophoretic Mobility Mean : -0.000340 cm<sup>2</sup>/Vs

**Figure 6.** Zeta-potential analysis of UC-MSC-derived exosomes (two independent replicates).

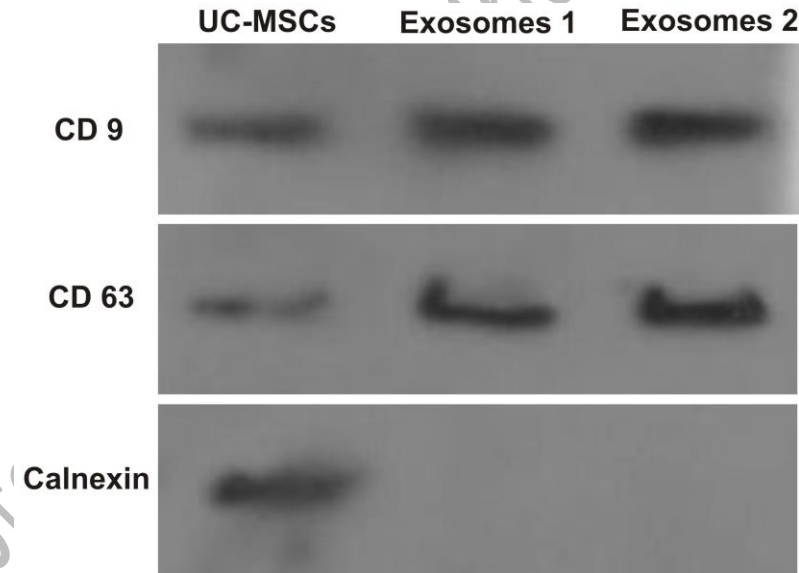


**Figure 7.** Western blot analysis of exosomal and cellular markers; Lane 1 (left side) corresponds to the whole cell lysate (Cell), and lanes 2 (middle) and 3 (right side) represent two technical replicates of exosomes (Exosomes 1 and Exosomes 2) isolated from the same batch of UC-MSC-conditioned medium.